




Proglacial lake evolution coincident with glacier dynamics in the frontal zone of Kvíárjökull, South-East Iceland

Jan Kavan^{1,2,3}  | Radim Stuchlík¹ | Jonathan L. Carrivick⁴  | Martin Hanáček¹ | Christopher D. Stringer⁴ | Matěj Roman^{1,5} | Jakub Holuša¹  | Pavla Dagsson-Waldhauserová^{6,7} | Kamil Láška¹ | Daniel Nývlt¹

¹Polar-Geo Lab, Faculty of Science, Masaryk University, Brno, Czechia

²Alfred Jahn Cold Regions Research Centre, Institute of Geography and Regional Development, University of Wrocław, Wrocław, Poland

³Centre for Polar Ecology, Faculty of Science, University of South Bohemia, České Budějovice, Czechia

⁴School of Geography and water@leeds, University of Leeds, Leeds, West Yorkshire, UK

⁵Centre for Glaciology, Department of Geography and Earth Science, Aberystwyth University, Aberystwyth, Wales, UK

⁶Agricultural University of Iceland, Borgarnes, Iceland

⁷Czech University of Life Sciences Prague, Prague, Czechia

Correspondence

Jan Kavan, Polar-Geo Lab, Faculty of Science, Masaryk University, Kotlarska 2, 611 37 Brno, Czechia.
Email: jan.kavan.cb@gmail.com

Funding information

Masaryk University, Grant/Award Numbers: MUNI/G/1540/2019, MUNI/A/1393/2021; EEA Grants, Grant/Award Number: EHP-CZ-ICP-1-003; Norwegian Financial Mechanism 2014–2021: SVELTA—Svalbard Delta Systems Under Warming Climate, Grant/Award Number: UMO-2020/37/K/ST10/02852; Natural Environment Research Council, Grant/Award Number: NE/S007458/1; Czech Science Foundation, Grant/Award Number: 22-206210; Rannis, Grant/Award Number: 207057-051; Orkurannsóknasjóður

Abstract

The termini of Icelandic glaciers are highly dynamic environments. Pronounced changes in frontal ablation in recent years have consequently changed ice dynamics. In this study, we reveal the inter-seasonal dynamics of the Kvíárjökull ablation zone and proglacial zone using ArcticDEM and Sentinel-2 images acquired between 2011 and 2021 and intra-seasonal dynamics with repeated UAV surveys during summer 2021. Average glacier surface velocity in the ablation zone ranged from 51 m year^{−1} in 2015 up to 199 m year^{−1} in 2018, with maxima within the axial zone of the glacier and minima on the glacier edges. Coincidentally, and in accordance with glacier retreat/advance, the ice-marginal proglacial lake fluctuated in its area, and we interpret that it was also a key factor in the development of the glacier terminus morphology. A complex spatial pattern of glacier surface elevation changes, including thickening in the frontal true left margin of the terminus, is interpreted to be due to variable subglacial topography, relatively fast ice flow from the accumulation zone and an insulating effect of glacier surface debris cover. In contrast, the true right (southern) part of the glacier terminus experienced thinning and retreat/disintegration also during the 2021 summer season, which we attribute to enhanced frontal ablation connected to the intrusion of lake water into the crevassed glacier terminus. Overall, this study suggests that where glaciers are developing ice-marginal lakes complex patterns of glacier dynamics and mass loss can be expected, which will confound understanding of the short-term evolution of these environments.

KEYWORDS

ablation zone, glacial lakes, ice flow velocity, surface elevation changes

1 | INTRODUCTION

Glaciers and ice caps have been losing mass at an enhanced rate during the 21st century across the globe (Hugonnet et al., 2021; Millan et al., 2022) because of atmospheric and oceanic warming. This has profound implications for marine and lacustrine ecosystems (Arrigo

et al., 2017; García-Rodríguez et al., 2021), as well as having a multitude of socio-economic impacts. Additionally, glacier retreat can alter the frequency and severity of natural hazards (Motschmann et al., 2020), particularly with respect to the formation and evolution of glacial lakes (Carrivick & Tweed, 2013) and glacier lake outburst floods (GLOFs) (Carrivick & Tweed, 2016). Glacier evolution and lake

This is an open access article under the terms of the [Creative Commons Attribution](https://creativecommons.org/licenses/by/4.0/) License, which permits use, distribution and reproduction in any medium, provided the original work is properly cited.

© 2024 The Authors. *Earth Surface Processes and Landforms* published by John Wiley & Sons Ltd.

evolution both affect how water resources are managed (Immerzeel et al., 2014). Glaciers with terminus lakes tend to have faster-flowing ice and higher rates of mass loss (Carrivick et al., 2020; Carrivick et al., 2022; King et al., 2018; Sutherland et al., 2020).

Icelandic glaciers and ice caps are of particular interest because they contain a disproportionately large amount of Europe's freshwater resources, with some of the thickest glaciers in the world (Immerzeel et al., 2014). This resource is of great importance for the people of Iceland because 73% of their electricity is sourced from hydropower (Hjaltason et al., 2018). Additionally, the tourism sector in Iceland is beginning to suffer the consequences of retreating glaciers, as accessibility to some sites is becoming more challenging (Welling & Abegg, 2021). This access challenge is concerning because tourism contributes to 8% of Iceland's GDP (Statistics Iceland, 2021). To best manage Iceland's water and energy security, as well as its economic prosperity, research into Icelandic glacier dynamics is essential.

Like glaciers and ice caps worldwide, Iceland's glaciers have been in continual decline since the Little Ice Age (LIA), except for a cool period between 1980 and 1993, when a glacier mass gain of 1.5 ± 1 Gt year⁻¹ was recorded (Björnsson et al., 2013). In recent decades, this rate of decline has increased, with half of the total mass loss since the LIA having occurred since 1994 (Aðalgeirsdóttir et al., 2020). Although Iceland is particularly susceptible to ice mass loss, as the effects of climate change are amplified in polar regions (Holland & Bitz, 2003), the rate of deglaciation has been reduced since 2011 as a result of North Atlantic regional cooling (Noël et al., 2022). Iceland's volcanic activity also plays an important role in controlling glacier retreat, with volcanic dust and tephra affecting the albedo of ice caps and geothermal activity contributing to subglacial melt (Aðalgeirsdóttir et al., 2020; Boy et al., 2019; Gunnarsson et al., 2020; Meinander et al., 2021; Möller et al., 2019). High precipitation rates across most of the southern Iceland (over 5000 mm year⁻¹) (Crochet et al., 2007) also further increase the dynamism of its glacial environment. Consequently, there are several different environmental factors, including natural climate variability, geothermal activity, high dust deposition rate and the complex topography of the glaciated terrain, that make Icelandic glacier dynamics especially complex to understand. Furthermore, that complexity is potentially exacerbated with the formation and evolution of ice-marginal lakes (Aðalgeirsdóttir et al., 2020). Ice-marginal lakes have formed across Iceland in recent decades (Baurley et al., 2020; Chandler et al., 2020a; Dell et al., 2019; Evans & Orton, 2015; Guðmundsson et al., 2019), but little is known about their short-term evolution and intra-seasonal dynamics and the control of the lake on glacier dynamics. The aim of this study is therefore to quantify the interannual trends and intra-seasonal variation in glacier dynamics in the vicinity of an ice-marginal lake.

1.1 | Study site

Kvíárjökull is one of Iceland's most dynamic glaciers, with spatially variable flow rates and heterogeneous ice surfaces that are prone to degradation (Phillips et al., 2017). Kvíárjökull flows from the southeast of the Vatnajökull ice cap in southeast Iceland (Figure 1a,b). The accumulation area (Figure 1c, A) is positioned at an altitude of approximately 1800–1900 m a.s.l. and the glacier snout flows towards the coastal plain (Figure 1c, Co), almost at the sea level. The LIA maximum extent

of Kvíárjökull was in the mid-18th century, and there was little change in its extent until the 1880s (Hannesdóttir et al., 2015a). Using aerial photography, Bennett et al. (2010) described the evolution of the glacier system since the 1940s and identified periods of hiatus that punctuate an overall trend of retreat. The lateral moraines are reported to be the biggest in Iceland (Thórarinnsson, 1956) and are most likely due to high rates of debris turnover (Eyles, 1979), with that debris sourced from steep volcanic rock walls positioned alongside the glacier terminus. These lateral moraines are interpreted to have originated during the Neoglacial, around 3200 yr BP (Spedding & Evans, 2002). During that time, the two major former meltwater outlets that cut through the lateral moraines in both the northern (Figure 1c, On) and southern (Figure 1c, Os) parts of the glacier were formed. The present position of these outlets is now several tens of metres above the present-day glacier surface. The current outlet passes through the moraine and is located in the east (Figure 1c, Oe). The water flowing out of the glacier is first stored in an ice-marginal lake and then drains through the moraine towards the sea (approximately 2 km away).

The present glacier foreland, bounded by its Neoglacial moraines, is predominantly composed of glaciofluvial sediments that have aggraded sufficiently to partially bury the downwasting glacier terminus. The ice is supplied from the accumulation zone through a relatively narrow corridor (700–900 m wide, approx. 2500 m long) located along the central axis of the glacier, resulting in relatively high flow velocities (Phillips et al., 2017). Unlike the central part, the margins are relatively stable with low flow velocities, especially in its frontal zone. A number of intermittent proglacial lakes were formed in the glacier foreland as a result of downwasting of ice-cored moraines throughout the 20th century, although none were reported to have formed on the foreland in 1998 (Bennett et al., 2010). Ice mass loss has driven the formation of the present lake and the expansion of that especially in the left lateral zone (Figure 1d,e) of the glacier since 2003 (Bennett et al., 2010).

2 | MATERIALS AND METHODS

A set of remote sensing data was used to describe glacier surface elevation changes, ice flow velocity and areal fluctuation of the ice-marginal lake between 2011 and 2021. This was complemented by more detailed study of glacier intra-seasonal dynamics in the summer 2021.

2.1 | Datasets

2.1.1 | Satellite images

We used satellite-derived data to calculate interannual and inter-seasonal changes in glacier velocity (see Section 2.2), to measure changes in glacier surface elevation (Section 2.3) and to delimit lake area (Section 2.4). For the period 2011 to 2016, we used 2 m resolution ArcticDEM strips downloaded from the Polar Geospatial Data Center at the University of Minnesota (Porter et al., 2018). From 2016 to 2021, we used Sentinel-2 (MultiSpectral Instrument, MSI) images downloaded from SentinelHub. To derive lake area between 2010 and 2015 we used Landsat-7 (Enhance Thematic Mapper plus,

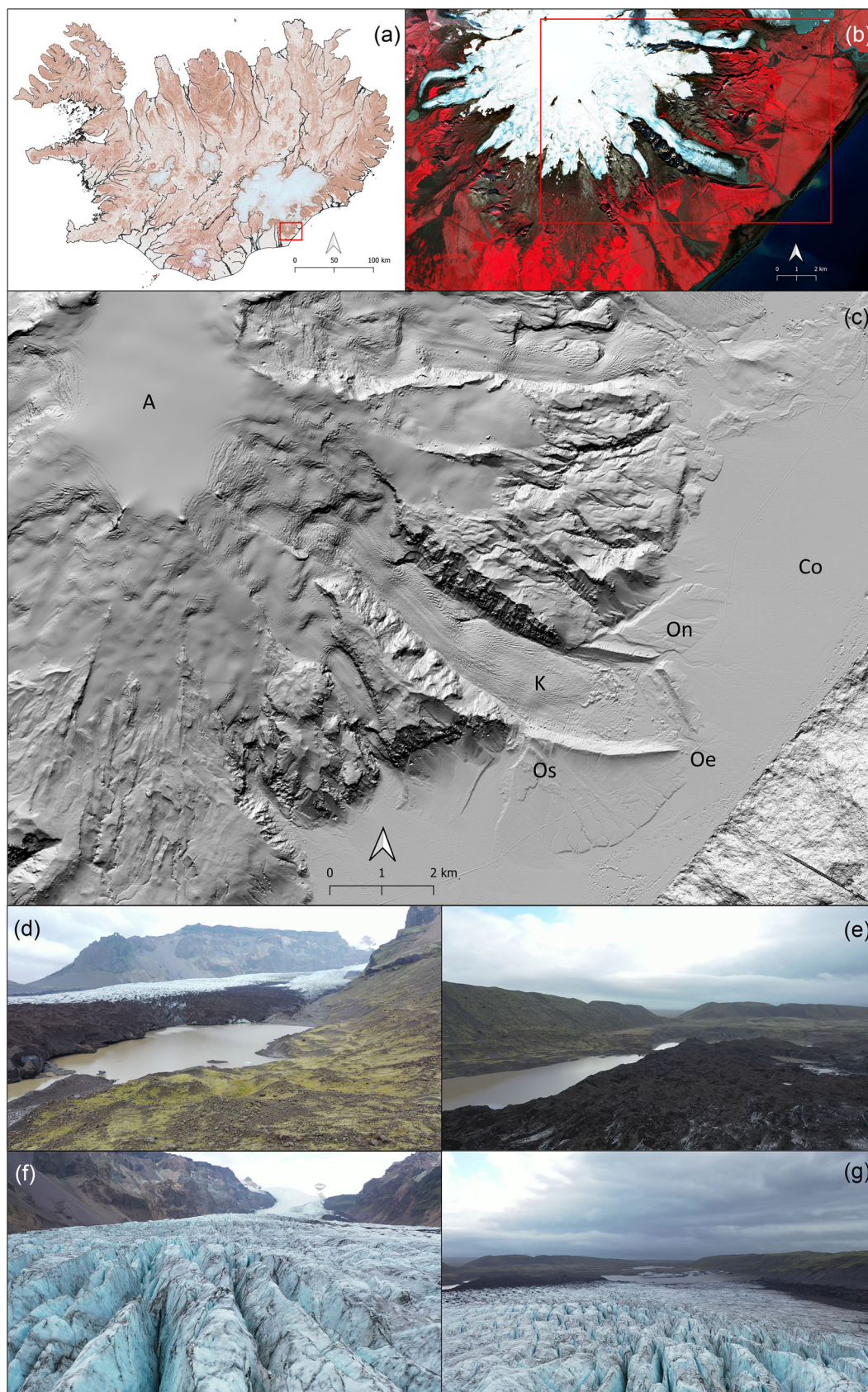


FIGURE 1 (a) Kviárjökull location within Iceland; (b) close-up view of the Kviárjökull area as seen on a Sentinel-2 false colour image (10 September 2021); (c) the DEM of the glacier and its immediate surrounding based on an ArcticDEM strip from 22.09.2011 (gaps filled by data from 06.10.2012); A = accumulation zone; K = Kviárjökull terminus; Co = coastal plain; On = glacier meltwater outlet north; Oe = glacier meltwater outlet east; Os = glacier meltwater outlet south; (d) UAV view on the northern part of the lake with the debris covered lateral part of the glacier from the stabilised Neoglacial lateral moraine; (e) the debris covered glacier surface with large supraglacial lakes—northern part; (f) massive crevasses in the narrow corridor connecting the ice cap on top of the image; (g) with the frontal part glacier and the lake. [Color figure can be viewed at wileyonlinelibrary.com]

ETM+) and Landsat-8 (Optical Land Imager, OLI) images, also from SentinelHub.

2.1.2 | UAV images

We conducted two UAV campaigns: (i) 28 to 29 June 2021 and (ii) 2 September 2021 to understand intra-seasonal dynamics. Both UAV campaigns used a DJI Mavic 2 Pro quadcopter equipped with a Hasselblad L1D-20c camera. The physical focal length of the camera is 10.37 mm (focal length 28 mm in 35 mm format equivalent). The camera has a 1" CMOS sensor, 20 million effective pixels, and is mounted on a three-axis gimbal. Although the UAV has a GNSS sensor, we found it to be imprecise. Therefore, we used several ground control points (GCPs). To ensure the GCPs were stable and not removed by strong wind, we used large stand-alone rocks that we could easily identify from the image. This had the added benefit that it prevented the pollution that lost artificial GCPs would cause. We measured the position of each GCP before each measurement with a Trimble GeoExplorer 6000 Series: Geo XH 3.5G, 120. We processed these data in the Trimble GPS Pathfinder Office software, and this showed us that the GCPs had not moved.

Overall, we flew 10 survey flights in each campaign that ensured the complete coverage of the frontal part of the glacier and its direct surroundings. A single flight lasted ~20 min, and the flight parameters and automatic flight plan were produced using the DJI GO 4 and Pix4Dcapture software. The camera and flight parameters are summarised in Table 1. We captured 2432 images during the June campaign and 2476 images during the September campaign.

2.2 | Glacier velocity

We used both manual and automatic approaches to calculate glacier ice velocity. The manual method entailed us inspecting the change in position of 20 reference points between pairs of images. We conducted this using ArcticDEM (2011–2016) and Sentinel-2 (2016–2021) images. This was complemented by annual ice flow velocity (automatic approach) derived from Sentinel-1 SAR data produced by ENVEO (<https://cryoportal.enveo.at/project/CISIM/>). More detailed information on the ice flow velocity product can be found in Wuite

et al. (2022). We extracted the average value for the whole glacier area as defined by Randolph Glacier Inventory version 6 (RGI Consortium, 2017) for each of the years studied.

Using the existing dataset provides us with more accurate picture of the spatial variability of the ice flow velocities, whereas the manual approach enabled us to prolong the time series prior to the SAR Sentinel-1 images, that is, prior to 2014.

2.3 | Interannual surface elevation changes

We defined two stable areas in the direct neighbourhood of the glacier for comparison, we used individual pairs of digital elevation models (DEMs) to analyse surface elevation change. The overall size of the two selected stable areas was approximately 1 km². The maximum difference between these DEMs in Z-coordinate was 0.105 m. We have summarised the stable area z-coordinate (elevations) differences between individual DEMs in Table 2.

Two ArcticDEM strips with the most complete coverage were used to evaluate long-term surface elevation changes. We used the data from 6 October 2012 and 19 March 2016.

2.4 | Changes in lake area

We used the optical satellite images to manually delineate the areal changes of the Kvíárjökull ice-marginal lake. For the pre-Sentinel era (2010–2015), we used Landsat-7 and Landsat-8 images, with the higher resolution Sentinel-2 images used for the 2016–2021 period. The manual measurement of the lake area contains error related to the resolution of the original image. We assume that the Sentinel-2 (10 m resolution) manual delineation contains an error of + – 5 m; similarly, the Landsat-7 and Landsat-8 (30 m resolution) contains an error of + – 15 m. As a result, the total uncertainty of the lake area time series can be estimated by accounting for error propagation to be on average 0.024 km². This corresponds to approximately 4% relative error when considering the lake area to fluctuate around 0.6 km² (see Section 3). For all interannual comparisons and analyses, we used images taken in the end of August or beginning of September.

2.5 | Glacier and lake intra-seasonal dynamics

We processed the UAV images using the structure from motion (SfM) method in Agisoft Metashape to produce 2.5D and 3D models from our set of 2D images (Özyeşil et al., 2017). We conducted a quality

TABLE 1 Camera and flight parameters (UAV campaigns).

Camera parameters	Flight parameters
Camera maker: Hasselblad	Flight height: approx. 120 m
Camera model: L1D-20c	Size of area: approx. 1600 × 1300 m
Camera angle: 90°	Forward/side overlap: 80%/72%
Still Image size: 5472 × 3648 pix.	Type of scan: single grid
Resolution: 72 dpi	GSD: approx. 0.028 m
F-stop: f/4.0–f/2.8	Speed: approx. 3 ms ⁻¹
Exposure time: 1/200 s	Time (only sensing): approx. 20 min
ISO: 100	Flight mode: automatic

TABLE 2 Differences in Z-coordinates (elevations) within stable areas.

Year	Difference [m]
2017–2016	–0.092
2016–2015	0.105
2015–2013	–0.021
2013–2012	0.017
2012–2011	0.057

control of all images in Agisoft before the analysis itself. Of the 4908 images acquired, we found 109 to be of poor quality due to feeble blur. These were all from the June campaign. However, we still incorporated these images as they occurred in a single narrow strip and their removal would have resulted in a 'no data' strip in the resulting model.

We then generated a sparse point cloud from the images using the GNSS on board the UAV. We used key and tie points from across the dataset, and manually corrected the location of the GCPs, to ensure the images were well aligned and accurate. We also improved the final accuracy of the model by incorporating the calibration properties of the camera. Finally, we created a dense point cloud and generated a texture to produce a DEM for each campaign. We then subtracted the DEM from the September campaign from the June campaign DEM to assess changes in glacier surface elevation during this period. The final parameters of the models are shown in Table 3.

We also visually inspected the UAV orthophotos to identify changes in the glacier-lake margin and changes in the adjacent proglacial areas.

2.6 | Methodology and accuracy issues

Using a combination of different remote sensing products (ArcticDEM, Sentinel-2, UAV) has proved to be a useful approach for describing the dynamics of the frontal part of a glacier. Most of the previous studies detecting high spatial and temporal resolution glacier changes worldwide used a single data source (e.g. Barr et al., 2018 in Kamchatka; Małeck, 2021 in Svalbard; Immerzeel et al., 2014 in Himalaya; Wang et al., 2021 in Tien Shan; or Ioli et al., 2022 in the Alps). However, these datasets are usually only available for a limited time; therefore, a combination of different data sources is usually used for long-term studies (e.g. Belart et al., 2019 in Iceland; Kavan et al., 2022 in Svalbard; Albedyll et al., 2018 in Greenland). Apart from airborne images, time-lapse photography has appeared as a powerful tool for analysing glacier-related processes in high temporal resolution (e.g. How et al., 2019; Mallalieu et al., 2017; Taylor et al., 2023). Oblique aerial or even terrestrial historic photographs might also be used for the reconstruction of early 20th-century glacier

TABLE 3 Final parameters of computed models. Processing machine parameters: CPU, Intel Core i7-8750H, 2.20GHz, 6 Cores, 12 Logical Processors; RAM, 16 GB; GPU, nVidia GeForce GTX 1060 with Max-Q Design, 6 GB.

	June campaign	September campaign
Involved images	2336	2426
Involved GCPs	14	14
Sparse point cloud	4 770 503	7 692 576
Dense point cloud	182 043 255	230 479 851
Number of faces	35 219 766	45 579 980
Orthophoto resolution [m]	0.05	0.05
DEM resolution [m]	0.05	0.05
RMSE [m]	0.113	0.345
Computing time [h]	Approx. 23	Approx. 17

characteristics where more appropriate image material is lacking (Bjork et al., 2012; Girod et al., 2018; Holmlund & Holmlund, 2019; Kavan, 2020). Here, we took advantage of multitemporal images and DEMs available within the last decade and combined them to obtain a complex view of the Kvíárjökull glacier front, including retreat rate, surface elevation changes, ice flow velocity, ice-marginal lake evolution and the development of different geomorphic features in the proglacial zone. A comparison of ArcticDEM individual strips was a simple and effective way to analyse surface elevation change and resulted in low errors (see Table 1). The GCPs used for UAV campaigns were not equally distributed because of the inaccessibility of the glacier surface. The GCPs were located in the glacier margins and proglacial zone. While this may result in high absolute elevation errors, especially in the central part of the glacier that was the most distant from the GCPs, the error is consistent between both UAV campaigns. Similar constraints with unequal distribution of GCPs when studying glacier surface changes are relatively frequent (e.g. Fugazza et al., 2018; Immerzeel et al., 2014; Wang et al., 2021). The accuracy of the DEM decreases with the distance to the closest GCP. Gindraux et al. (2017) found the rate of accuracy decrease typically of 0.09 m per 100-m distance over a glacier surface. This means in our case that the vertical error in the centre of the glacier (about 1000 m from the nearest GCP) could be about 1 m. We argue that the heterogeneous nature of the glacier surface with crevasses and other visible distinctive features (Figures 1, 6 and 8) has been favourable in terms of precision of the point cloud generation. Despite that, it is necessary to be cautious when interpreting changes in the central part of the study area where the uncertainties are largest.

3 | RESULTS

3.1 | Lake surface area

Stable hydrological conditions were observed between 2010 and 2011, followed by a significant increase in areal extent between 2011 and 2012 (from 0.43 to 0.66 km² i.e. 35% increase) following a 200-m retreat of the glacier terminus in the southern part of the glacier terminus (Figure 2b). Since 2012, the lake area has been mostly stable; fluctuating around 0.6 km². However, the ice-marginal length has been highly variable over the same period. This variability coincides with the retreat and advance of the glacier terminus and is particularly evident in the southern part. The northern part of the lake shore is more stable, likely due to thicker ice and consequently well-stabilised grounded glacier terminus. The lake shoreline adjacent to the frontal moraine is relatively stable, which we interpret to be due to the presence of vegetation, which has consolidated sediments. Some other minor changes in shoreline position likely occurred due to local slope deformation in steep parts of the shore.

3.2 | Surface elevation changes in 2012–2016

A general thickening (Figure 3) occurred over much of the glacier. Thinning was largely confined to the southeastern sector of the frontal zone ('SE' in Figure 3), which is rather flat and subjected to frequent calving (as seen, e.g. from Sentinel images in Figure 4b). The

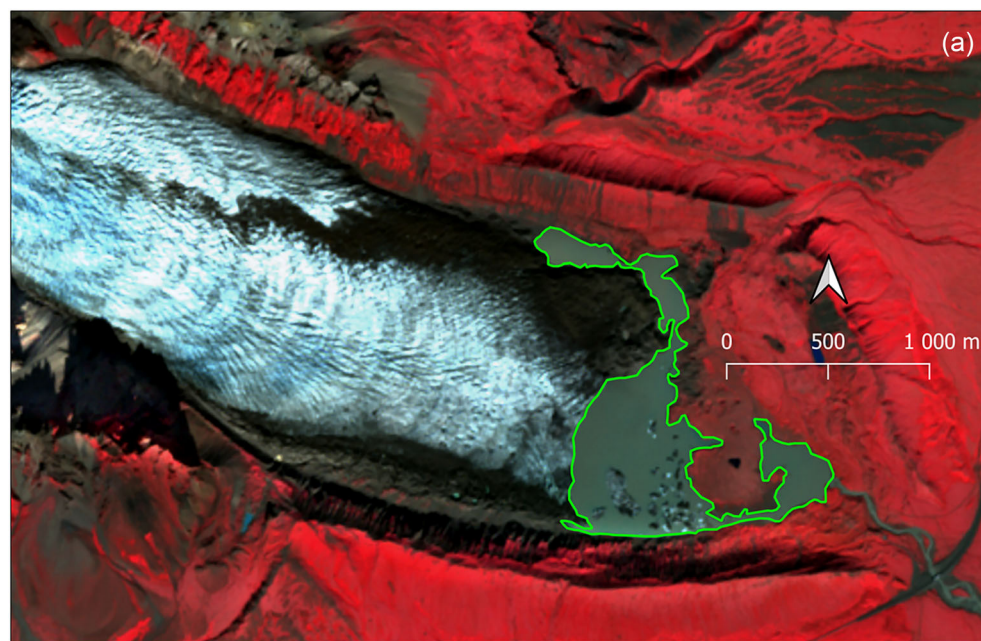


FIGURE 2 Glacier terminus retreat/advance resulted in changes of lake outline and also areal extent; (a) the situation of the lake as seen from Sentinel-2 image (10 September 2021) with the lake extent highlighted in green; (b) average ice flow velocity (both manually estimated and SAR derived), lake areal extent and ice-contact length evolution from 2010 to 2021. [Color figure can be viewed at [wileyonlinelibrary.com](https://onlinelibrary.wiley.com/doi/10.1002/esp.2781)]

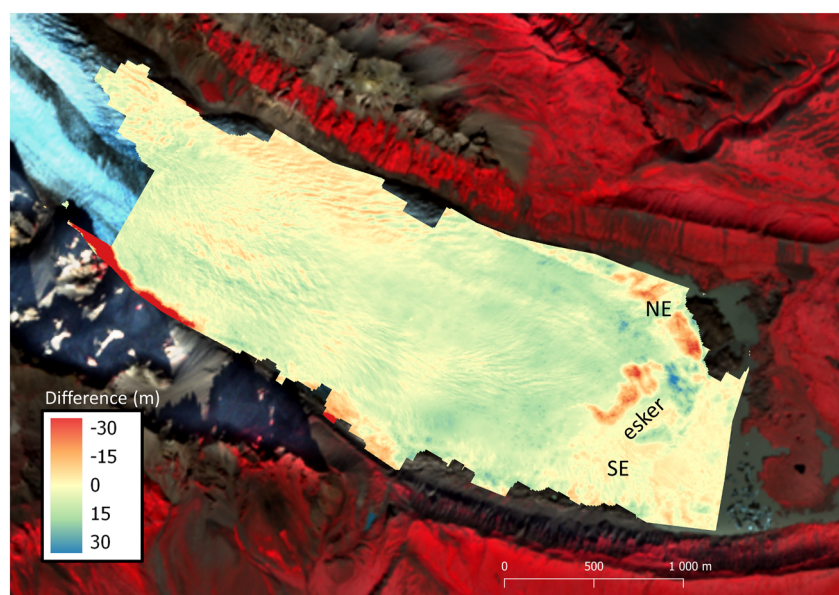
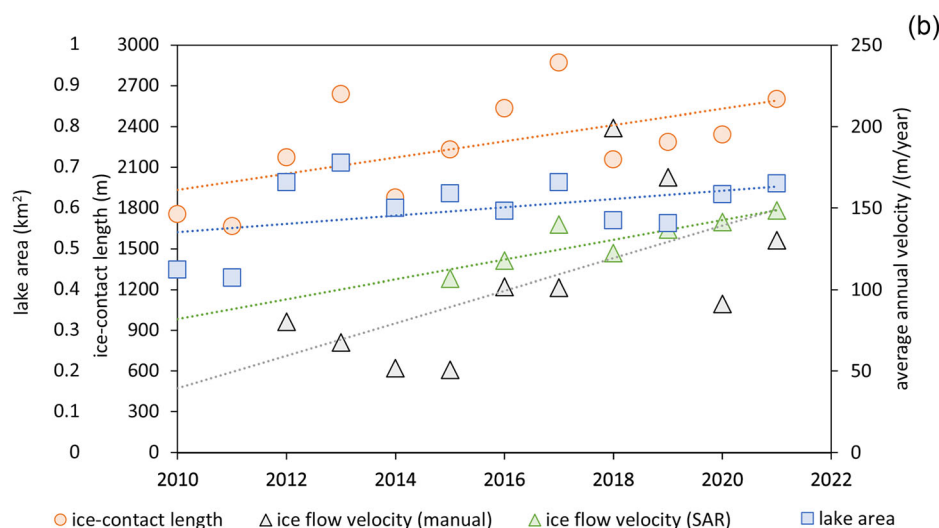


FIGURE 3 Comparison of the 2012 and 2016 ArcticDEM strips with the resulting difference model; the coloured scale expresses the elevation change in metres between 2012 and 2016 DEMs; the difference model is masked to the glacier extent, with the Sentinel-2 image (31/08/2021) used as a background. [Color figure can be viewed at [wileyonlinelibrary.com](https://onlinelibrary.wiley.com/doi/10.1002/esp.2781)]

northern part of the frontal sector ('NE' in Figure 3) had a very uneven surface in both years (2012 and 2016), and the resulting changes were very spatially variable, with thickening in some places

and thinning in others. A similar spatial pattern was observed in the case of the moving esker (marked as 'esker' in Figure 3 and identified by Phillips et al., 2017). As a result, the shape of the esker is very

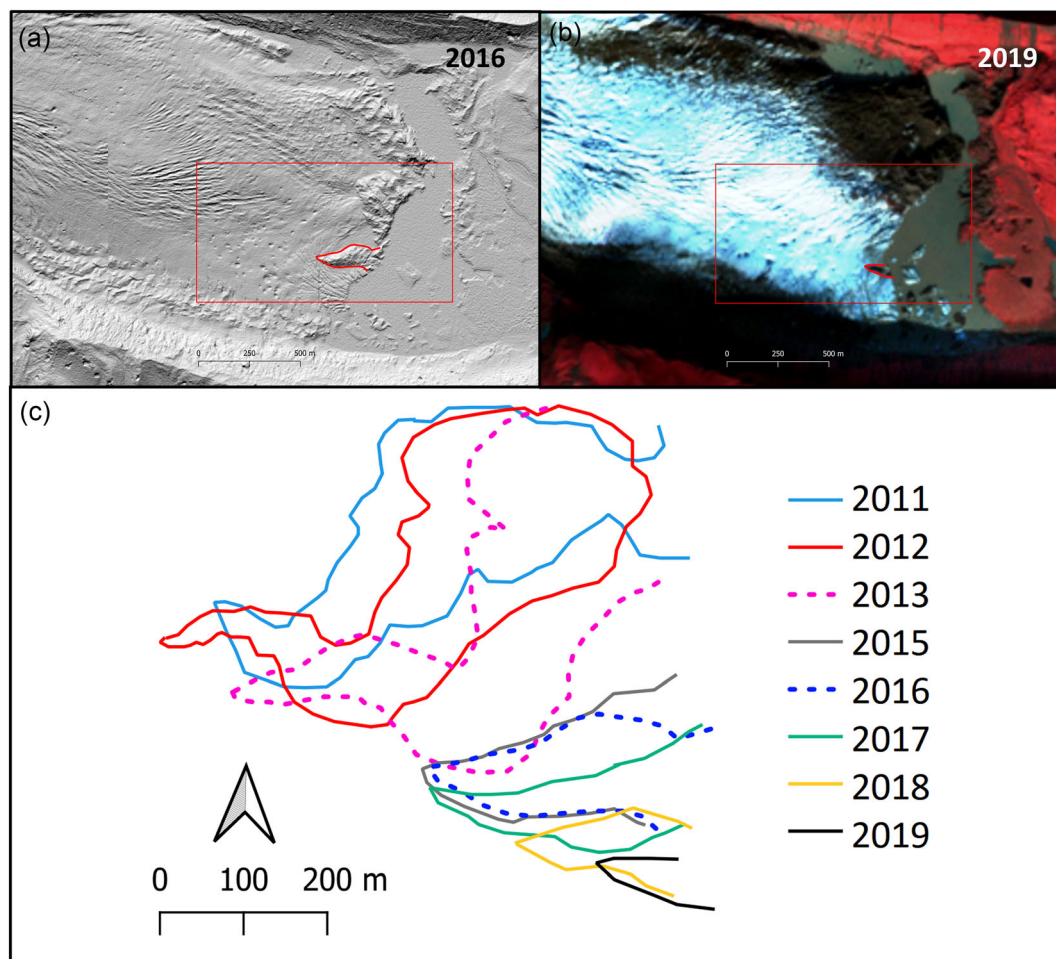


FIGURE 4 Movement of the ice-cored esker in the central part of the glacier front as seen from ArcticDEMs (a) and Sentinel-2 images (b) (2011–2019); (c) interannual evolution of the esker shape and position. [Color figure can be viewed at [wileyonlinelibrary.com](https://onlinelibrary.wiley.com/doi/10.1002/esp.2781)]

clearly identifiable on both DEMs and the final difference model. This makes the esker a good marker for observing glacier movement, as the changes in surface elevation highlight that the glacier has moved from its 2012 position, as highlighted by the loss of elevation in this region.

3.3 | Glacier surface velocity

Average glacier surface velocity at the glacier terminus was $104.3 \text{ m year}^{-1}$ in the period 2012–2022. The velocity was, however, rather variable and was relatively low in the early part of the observation period, followed by a large increase in velocity in 2018 and 2019. We recorded the minimum surface velocity (51 m year^{-1}) in 2015 and the maximum in 2018 (199 m year^{-1}) (Figure 2b). The average velocity derived from Sentinel-1 SAR images (Wuite et al., 2022) is more homogeneous but still within the values obtained by manual measurement (Figure 2b).

We observed the maximum velocity in the upper reaches of the glacier, where the ice surface gradient is greatest (15° in average) and the glacier is most constrained through a narrow corridor (700–900 m). This terrain configuration likely enhances the downward movement of the glacier. In the lower reaches, we observed a low

ice flow velocity (see Figure 5). A possible mechanism for this is that the mass of the ice is less constrained close to the terminus, thus reducing the stress on the ice and consequently reducing its velocity.

The fact that ice flow velocities follow a transverse profile, that is, the highest velocities in the centreline compared to the lateral zones (Figure 5), suggests the importance of internal deformation of the ice mass (Jennings & Hambrey, 2021). The highest flow velocities occur in the areas where there is sufficient mass/pressure from upper parts of the glacier to cause deformation. We saw this expressed by numerous crevasses in the central part of the narrow corridor (Figure 1f). The frontal part of the glacier, where the ice flow velocity decreases, is relatively flat and the surface is homogeneous without significant crevassing (compare with Figure 6a,b).

3.4 | 2021 ablation season dynamics

The relatively short period of observation from 28/29 June to 2 September 2021 was characterised by significant changes in the glacier terminus position, that is, glacier areal extent, surface elevation changes and changes in the adjacent proglacial geomorphology as a result of fluvial erosion.

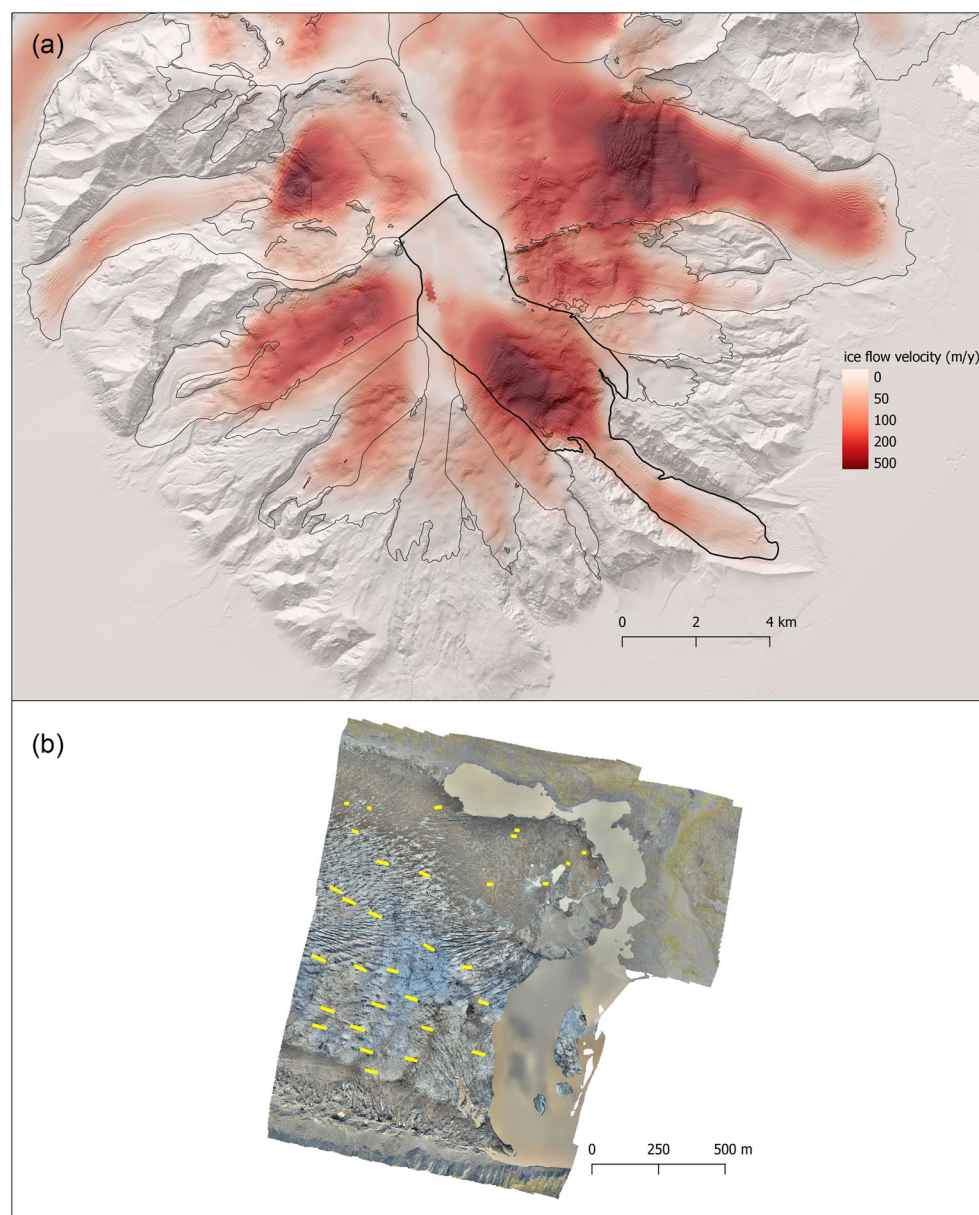


FIGURE 5 (a) Spatial pattern of ice flow velocity for Kvíárjökull and neighbouring glaciers (based on 2014–2021 Sentinel-1 SAR data produced by ENVEO; see chapter 2.2.), glacier outlines taken from RGI 6.0, Kvíárjökull highlighted in thick line; shaded relief derived from ArcticDEM used as background; (b) glacier movement between the two UAV campaigns in summer 2021 illustrated by the vectors of reference points displacement (in yellow). [Color figure can be viewed at [wileyonlinelibrary.com](https://onlinelibrary.wiley.com/doi/10.1002/esp.2781)] [wileyonlinelibrary.com](https://onlinelibrary.wiley.com/doi/10.1002/esp.2781)]

3.4.1 | Glacier areal extent changes

We identified the most pronounced changes in the southern part of the glacier terminus, close to the position of the calving front. A relatively large part of the glacier had disintegrated between the two UAV campaigns, which resulted in a retreat of more than 100 m in the most pronounced case (Figure 6c). The northern part of the frontal zone was stable and we only observed minor changes caused by lateral moraine slope failures following the thawing of ice-cored debris cover (Figure 6).

3.4.2 | Surface elevation changes

We saw a large thinning of the frontal part of the glacier (Figure 7). Despite the above-zero air temperatures with average 9.6°C between the two UAV campaigns (see Data S1) suggesting that melting, and therefore surface lowering, would be widespread across the entire frontal part, we observed a minor increase in surface elevation in its

northern margin. This is perhaps due to an inflow of ice from the higher portions of the glacier; an interpretation supported by our observation of slowdown of glacier movement in this zone (Figure 5b). The contrasting behaviour of the northern and southern glacier margins can be explained by the variation in lake depth across the glacier margin. The northern part of the glacier terminus sits on the bedrock, whereas the southern part is calving into the lake and is likely to be floating.

3.4.3 | Proglacial landform evolution

Changes in the morphology of the highly dynamic lateral and frontal zones of the glacier were both widespread and profound. In regions where the foreland is in direct contact with the glacier body, degradation of ice-cored lateral moraines, development of several new kettle lakes and enlargement of already existing lakes was observed (Figure 8h,i). The northern section of the glacier terminus has a large quantity of supraglacial debris. Consequently, this section has become

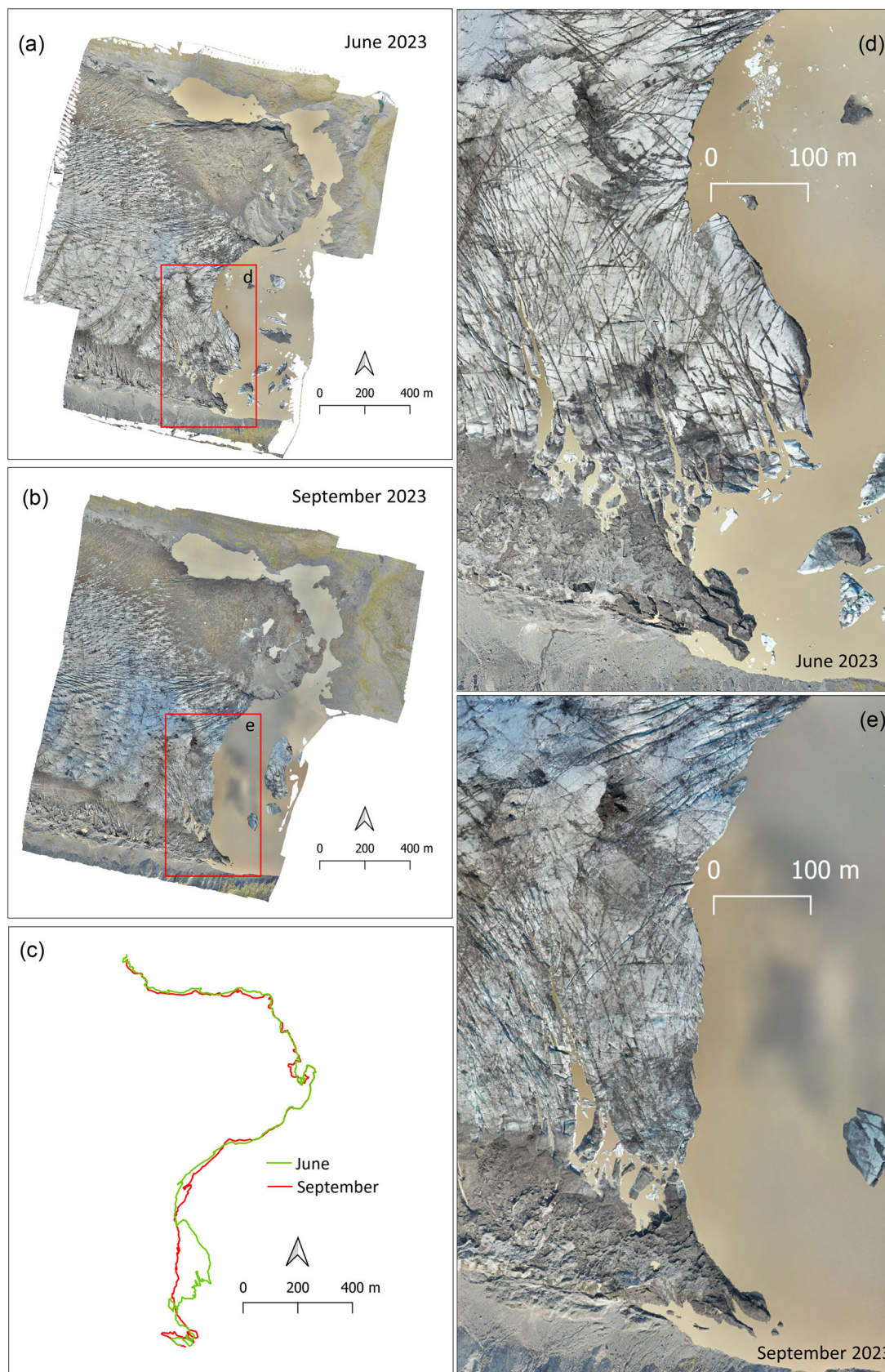


FIGURE 6 (a) Orthophoto map of the frontal glacier zone from 28/29 June 2021; (b) 2 September 2021; (c) outline of the glacier front overlapped to a single image; (d,e) detail view of the southern frontal zone to illustrate the lake water intrusion into the crevassed ice field. [Color figure can be viewed at [wileyonlinelibrary.com](https://onlinelibrary.wiley.com/doi/10.1002/esp.2781)]

more stable and has begun to transition from debris-covered glacier into ice-cored moraine, with slope processes becoming more important than glacier dynamics to the evolution of its morphology (Figure 8b,c).

We also observed a spatial variability in the formation of lakes and the development of meltwater channels (Figure 8f,g). The variability in supraglacial debris is a possible mechanism that could explain this heterogeneity. On the eastern shore of the lake, adjacent

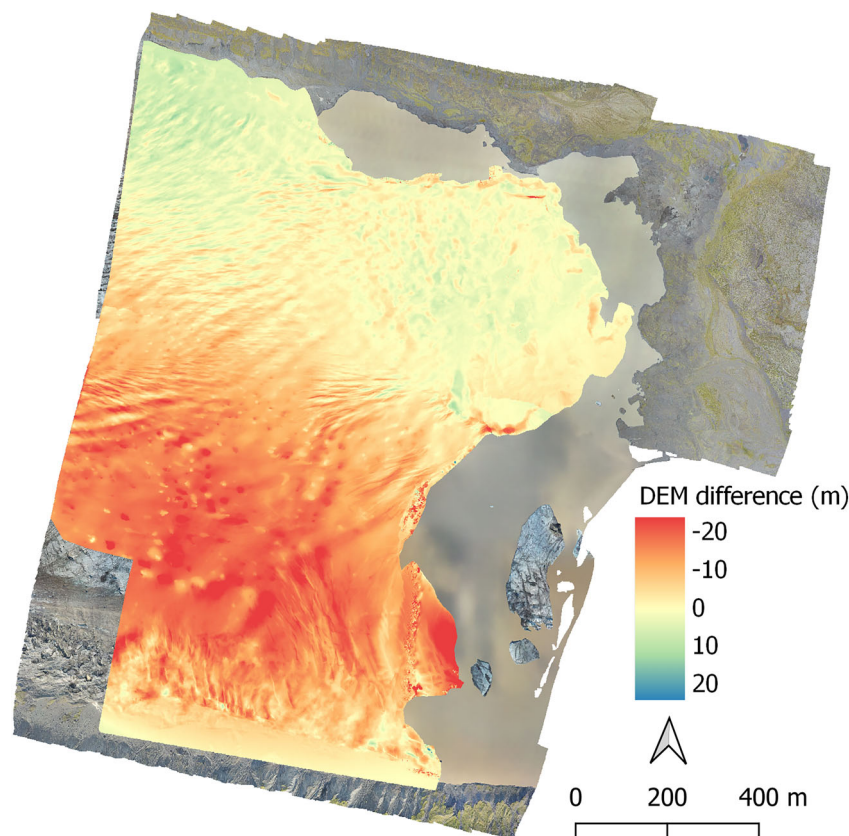


FIGURE 7 Surface elevation change between June and September 2021 based on the DEMs derived from UAV mapping campaigns; the background image is the orthophoto map from September 2021. [Color figure can be viewed at [wileyonlinelibrary.com](https://onlinelibrary.wiley.com/doi/10.1002/esp.2781)]

to the Neoglacial frontal moraine, we did not observe evidence of glacial erosion. However, mass movement affects the relatively steep shore zone, as illustrated in Figure 8d,e.

4 | DISCUSSION

4.1 | Glacier dynamics and lake interaction

Despite their importance on glacier movement, there is still some debate over the origin of the complex system of crevasses on Kvíárjökull. Phillips et al. (2017) presented a model of the active axial zone of the glacier surrounded by lateral and latero-terminal parts with slow movement. The active axial zone is not moving as a whole, but rather as individual sections with surge-like movements. These complicated shear stress processes inside the glacier led to the development of a strike-slip shear zone in the termino-glacial zone and the clockwise rotation of the ice-cored esker into its concertino shape deformation (as described by Knudsen, 1995). However, Swift & Jones (2018) did not agree with this mechanism and suggested that the driving mechanism for glacier flow, surface crevassing and shape deformations reflect the complex subglacial topography.

We argue that another important driving factor on glacier dynamics is the ice-marginal lake itself, especially its southern basin. The lake shoreline evolution shows that the northern part of the glacier advanced to its northeastern forefield about 5–6 years after the abrupt extension of the lake (Figure 2b). It therefore appears that the lake expansion caused a speed-up of glacier thinning and eventually complete disintegration of the southern latero-terminal glacier zone adjacent to the active axial zone, as defined by Phillips et al. (2017). The thermo-mechanical processes by which the lake promoted glacier

thinning and ice margin collapse cannot be elucidated by our study and are complex and interlinked (c.f. Carrivick et al., 2020). Propagation of lake water beneath and into the lowermost parts of the glacier is likely, for example, and would affect basal temperature, pressure and shear stress. What we can determine is that degradation of the passive lateral zone of the glacier created space for the active axial zone, which was, until then, blocked. The axial zone of the glacier consequently sped up its movement and advanced rapidly. The 5–6 years of delay was necessary for the degradation of the passive latero-terminal zone.

However, Phillips et al. (2017) identified the main pulses of flow as towards the northeast. In 2018, the glacier advanced towards the northeast, which resulted in the narrowing of the central part of the connection between its southern and northern basins. This movement supports the existence and activity of the longitudinal shear zone between the axial and latero-terminal zone of the terminus (as described by Phillips et al., 2017). The shear zone directed the advance of the axial zone to the northeast. In the absence of the shear zone, the glacier would probably advance in the direction of the main flowline (as described by Swift & Jones, 2018) to the present lake, where it would cause the major thrusting described in the 1990s (Bennett et al., 2010). Dell et al. (2019) identified similar dynamic behaviour in Fjallsjökull (a neighbouring glacier sharing a common ice cap as an accumulation area) with the existence of localised flow ‘corridors’, which conveyed relatively faster flow towards the glacier’s terminus. Spatially complex behaviour has also been attributed to site-specific factors, such as basal topography.

The stability of the shoreline adjacent to the Neoglacial frontal moraine contrasts with the variability of the shoreline adjacent to the glacier itself. We attribute many of the shoreline position changes adjacent to the glacier to the retreat and advance of the glacier

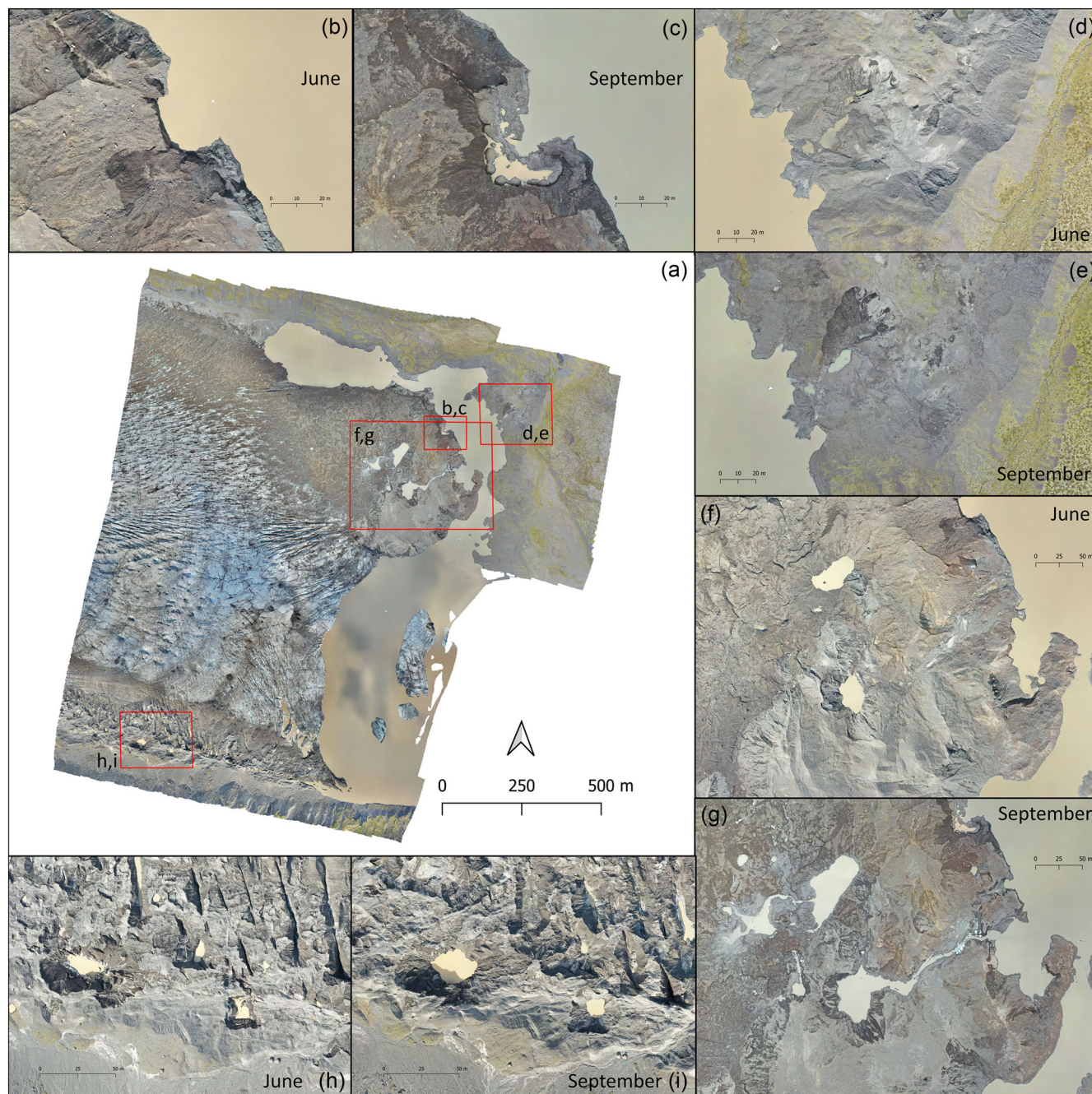


FIGURE 8 (a) Examples of the development of the proglacial zone during the 2021 ablation season; (b,c) the debris-covered northern part of the glacier terminus; (d,e) landslide activation on the steep (up to 20°) shoreline adjacent to the Neoglacial frontal moraine; (f,g) development of lakes on the surface of the debris-covered glacier front accompanied by the disintegration of the shoreline; (h,i) development of kettle lakes at the southern glacier margin. [Color figure can be viewed at [wileyonlinelibrary.com](https://onlinelibrary.wiley.com/doi/10.1002/esp.2781)]

(Figure 2). Such variable shoreline position has also been described in other Icelandic glaciers, such as at the Jökulsárlón ice-marginal lake, about 15 km from Kvíárjökull, where Baurley et al. (2020) reported an increase in lake areal extent of $\sim 20 \text{ km}^2$ since 1982 following a massive retreat of the glacier front of up to 3.5 km. Similarly, an ice-marginal lake has also increased in size significantly since a large readvance in the 1990s after which the retreat exceeded 35 m year^{-1} (Chandler et al., 2020b).

The ice-contact shoreline in the southern lake basin was uneven and jagged after 2012 because water inundated the complex system of cracks in the glacier front. This unusual shoreline morphology has also been recorded in previous iterations of the Kvíárjökull lake (1964,

1980, 2003, as described by Bennett et al., 2010) and we interpret this to mark the transition of the lake from supraglacial towards proglacial. This is contrasted by the northern lake, where the ice-contact shoreline is more even and stable, likely because it is bound by an ice-cored push moraine, which runs parallel to the lake shoreline (Phillips et al., 2017). These contrasting shorelines have been characteristic of the lakes since at least 2003 (Bennett et al., 2010) and persisted until 2020. As described in Figure 2b, the shoreline morphology changed following the calving of a large portion of ice in the southern lake, and this likely represents a shift in lake type, from supraglacial to ice-marginal, and calving has begun to be the leading process of frontal ablation along the whole southern ice-contact shoreline.

Kvíárjökull experienced several episodes of rapid advances between 1985 and 1990, followed by smaller advances between 1990 and 1998 (Phillips et al., 2017). Phillips et al. (2017) also describe that at the same time, the ice-marginal lake area fluctuated in front of the southern part of the glacier front. The lake has also previously partly inundated the flat and thin regions of the glacier front (c.f. Figure 6d,e), potentially destabilising the glacier front. The presence of the lake in the southern glacier forefield is facilitated by the existence of a bedrock overdeepening (Magnússon et al., 2012). The abrupt increase of lake areal extent in 2012–2013 was caused by inundating of the fan-shaped system of radial and concentric crevasses in the glacier marginal zone (south of the ice-cored esker). Lake expansion coincided with a slowdown of the glacier flow velocity. The glacier started to move towards the northeast in 2018 and this has resulted in the lake separating into two distinct basins: a small northern basin and a large southern basin (Figure 2b). A pulse of fast advance recorded in the period 2012–2013 (Phillips et al., 2017) occurred shortly after an important and abrupt expansion of the southern lake basin and the disintegration of the flat, thin marginal zone of the glacier.

Glaciers terminating in lakes often recede more rapidly than their land-terminating counterparts (e.g. Tsutaki et al., 2019) and lose mass by frontal ablation (Sutherland et al., 2020; Watson et al., 2020). Even though Kvíárjökull glacier presents similar characteristics to other lake-terminating glaciers, it does not follow this general trend, and we have found that its frontal position stays relatively stable as well as the surface elevation. We attribute this to high ice flow velocity bringing large ice masses towards its frontal margin. We observe the transfer of meltwater from the lake to the glacier, as is shown on the orthophoto (Figure 6d,e), where the intrusion of lake water into the crevassed glacier front is clear. The interaction between the lake and the glacier can further enhance some of the processes that are already in action. Baurley et al. (2020) emphasised that a calving front and the presence of lake water can accelerate the flow velocity of glaciers. This enhanced ice flow can be amplified by the presence of a deep reverse-sloping subglacial trough. This could happen Kvíárjökull in the future because its subglacial trough is relatively large and deep and further retreat of the glacier may lead to the formation of a $\sim 4 \text{ km}^2$ lake (Magnússon et al., 2012).

4.2 | Surface elevation change and mass balance

Most of the glaciers in Iceland have lost mass over the last two decades (Aðalgeirsdóttir et al., 2020). However, the frontal parts of Kvíárjökull do not appear to have followed this same trend. While parts of the glacier terminus have shown thinning between 2012 and 2016 (Figure 5), most of the area covered by our analysis is relatively stable or is increasing in thickness. Nevertheless, it is important to consider that the present-day surface morphology of the glacier is a product of both surface lowering, as a product of melt, and ice mass thickening, as a product of ice movement from the accumulation zone of the glacier. Consequently, the ice mass lost during positive air temperature in the summer is compensated for by an inflow of ice from the glacier's accumulation zone, thus leading to a long-term quasi-equilibrium state of the glacier terminus.

Most of the changes were directly related to the flow of the glacier and deformations of the ice mass (Phillips et al., 2017) due to the glacier overdeepening as reported by Magnússon et al. (2012) and steep reverse slope in the terminus zone (Phillips et al., 2017). It seems that the bedrock topography and continuous inflow of the mass from the upper parts of the glacier are the controlling factors of the surface elevation changes. The effect of climatic factors seems to be of second order as no systematic thinning was observed despite the increasing air temperatures (Figure 3). The accumulation-to-ablation ratio (AAR) of Kvíárjökull has a value of 0.64 (Hannesdóttir et al., 2015b), which is typical for Icelandic glaciers; however, the high turnover rate (Bradwell et al., 2013) means the ice flow still compensates for the high ablation (Eyles, 1979). This is confirmed by only 0.27 m year^{-1} of average surface lowering reported between 2010 and 2019 compared to 0.42 m year^{-1} on the neighbouring Fjallsjökull, 0.49 m year^{-1} on Svínafellsjökull or the Iceland average of 1.03 m year^{-1} (Hugonnet et al., 2021). The deformation of ice mass driven by bedrock topography results in the complex spatial pattern of surface elevation changes.

Calving is responsible for a substantial part of the overall mass loss of the glaciers in contact with lakes (Benn et al., 2007). At Kvíárjökull, calving was responsible for more than 100 m of glacier retreat during the 2021 summer season (Figure 6c). The interactions between the glacier and ice-marginal lake are quite complex and include multiple feedbacks with high spatiotemporal variability. As a result, this feedback may have led to enhanced melting of the frontal zone, especially through meltwater exchange and lake water temperature effects (Carrivick et al., 2020).

Another factor controlling surface elevation changes is debris cover. This affects the surface energy balance by providing the glacier surface with insulation when the layer exceeds a certain thickness (Ben-Yehoshua et al., 2020; Dragosics et al., 2016; Meinander et al., 2021; Nicholson & Benn, 2013), which can reduce surface melting. However, if debris cover is present in tandem with ice cliffs (Buri et al., 2016) and supraglacial ponds (Miles et al., 2017), the opposite effect may occur, with more pronounced melting as vertical surfaces are exposed. The northern part of the glacier front is covered by debris (Figure 1). This debris cover coincides with a thickening (Figure 7), similar to observations at Svínafellsjökull in 2021 (Ben-Yehoshua et al., 2020). It seems probable that the debris-covered part of the glacier was protected from surface melting between the two UAV campaigns in the summer of 2021, which resulted in the highly spatially variable glacier surface elevation change (pronounced lowering in the southern part and stability or even increase in the northern part). The substantial thinning in the southern part during 2021 summer was likely caused by extremely high air temperatures with the highest average summer air temperatures measured at several stations around Vatnajökull ($+3^\circ\text{C}$ anomaly in July and August relative to 2011–2020; IMO, 2022).

4.3 | Proglacial zone terrain alterations

The proglacial zone in direct contact with the glacier margin is often the most active in terms of terrain alterations (Carrivick et al., 2022). The rate of change in the ice-cored moraine is affected primarily by the angle of slopes and the presence of meltwater streams

(Ewertowski & Tomczyk, 2015). These complex factors are fully responsible for the development of the northern part of the glacier terminus. The degradation of dead ice within the LIA frontal moraine, which formed between 130 and 140 years ago, is likely to have ceased. Consequently, this landscape is beginning to stabilise and only minor slope processes can be detected in this region. Conversely, the lateral ice-cored moraines are affected by intense marginal meltwater and the stream often actively undercuts its slopes. The Neoglacial frontal moraine is not affected by these streams because of the presence of the proglacial lake, which redistributes the fluvial energy across the area of the lake and tempers the rate of erosion, limiting it to only downwasting and backwasting as a result of slow dead ice thawing (Kjær & Krüger, 2001). It is likely that without the lake, the frontal moraine would undergo more intense fluvial erosion with slope undercutting and probably lower the whole moraine ridge. We argue that the protection of the Neoglacial frontal moraine by the existence of the ice-marginal lake has helped to preserve the exceptionally large moraine ridge (e.g. Thórarinnsson, 1956). The only relatively active zone susceptible to erosion is the lake shoreline itself, where wave action is responsible for the destabilisation of the shore and has intensified slope movements. We identified erosion of the lake shoreline adjacent to the glacier during a single summer melt season, which others have also identified at glaciers in different parts of the world (e.g. Fu et al., 2022; Zhong et al., 2022). Here, the changes in the marginal zone are expressed in the formation of kettle lakes, or the widening of existing ones, as well as the activation of slope processes.

5 | CONCLUSIONS

Kvíárjökull is a glacier that has a complex topography, comprising a steep and narrow corridor connecting the accumulation area to the terminus, and is situated in a temperate region with high precipitation rates and high summer air temperatures. Consequently, this glacier system is highly dynamic and characterised by high ice flow velocity. This highly dynamic system has undergone varied rates of terminus retreat and glacier thinning, and these changes, along with ice flow velocities, coincide with the extent of its proglacial lake. Specifically, increased lake extent coincides with decreased glacier velocity. The disintegration of a large portion of ice in the southern lake in 2020 likely represents a shift in lake functioning. Calving has begun to be the leading process of frontal ablation along the whole southern ice-marginal lake shoreline.

The northern part of the glacier terminates on land and has a substantial debris cover. This part was stable without any significant surface thinning, even experiencing slight elevation increase (up to 5 m). The insulation effect of the debris cover and high input of ice mass from the accumulation zone probably compensates for the mass loss caused by high summer air temperatures. Conversely, the southern part of the glacier terminus lost up to 20 m from its surface elevation during the summer of 2021. The ice-marginal lake in the southern part introduced another mass loss process: calving, which we suggest explains the enhanced ice mass loss and ice velocities at the southern margin of the terminus. We also detected changes in the deglaciating foreland, where the formation and widening of kettle lakes and minor landslides were detected during the summer melt season of 2021.

In the future, the high ice flow velocities of (up to 200 m year⁻¹), combined with over-deepening in the bedrock topography that make lake expansion possible, may combine to accelerate glacier mass loss and retreat.

AUTHOR CONTRIBUTIONS

Conceptualisation: Jan Kavan and Daniel Nývlt. *Fieldwork:* Jan Kavan, Radim Stuchlík, Matěj Roman, Jakub Holuša and Daniel Nývlt. *Data processing:* Jan Kavan and Radim Stuchlík. *Writing—initial draft:* Jan Kavan, Radim Stuchlík, Martin Hanáček and Christopher D. Stringer. *Writing—reviewing and editing:* Jonathan L. Carrivick, Matěj Roman, Jakub Holuša, Pavla Dagsson-Waldhauserová, Kamil Láska and Daniel Nývlt. *Funding acquisition:* Jan Kavan and Kamil Láska.

ACKNOWLEDGEMENTS

This work was supported by the Masaryk University project EHP-CZ-ICP-1-003 funded from the EEA Grants mechanism and Masaryk University ARCTOS MU (MUNI/G/1540/2019) and MUNI/A/1393/2021. The research leading to these results has also received funding from the Norwegian Financial Mechanism 2014–2021: SVELTA—Svalbard Delta Systems Under Warming Climate (UMO-2020/37/K/ST10/02852) based at the University of Wrocław. CDS was in receipt of a PhD studentship from the Leeds-York-Hull Natural Environment Research Council (NERC) Doctoral Training Partnership (DTP) Panorama under grant no. NE/S007458/1. MR was supported from a Czech Science Foundation (GACR) grant 22-206210. PDW received a support from Icelandic Research Fund (Rannís) grant no. 207057-051 and Orkurannsóknasjóður (National Power Agency of Iceland). Open access publishing facilitated by Masarykova univerzita, as part of the Wiley - CzechELib agreement.

DATA AVAILABILITY STATEMENT

Satellite data used in the study are publicly available from Sentinel Hub (<https://www.sentinel-hub.com/>) and Polar Geospatial Center (<https://www.pgc.umn.edu/data/arcticdem/>). Ice flow velocity data are available from ENVEO (<https://cryoportalenveo.at/project/CISIM/>), and UAV-based data are available on request.

ORCID

Jan Kavan  <https://orcid.org/0000-0003-4524-3009>

Jonathan L. Carrivick  <https://orcid.org/0000-0002-9286-5348>

Jakub Holuša  <https://orcid.org/0000-0002-3255-2278>

REFERENCES

- Aðalgeirsdóttir, G., Magnússon, E., Pálsson, F., Thorsteinsson, T., Belart, J.M.C., Jóhannesson, T., et al. (2020) Glacier changes in Iceland from ~1890 to 2019. *Frontiers in Earth Science*, 8, 523646. Available from: <https://doi.org/10.3389/feart.2020.523646>
- Albedyll, L., Machguth, H., Nussbaumer, S.U. & Zemp, M. (2018) Elevation changes of the Holm land ice cap, northeast Greenland, from 1978 to 2012–2015, derived from high-resolution digital elevation models. *Arctic, Antarctic, and Alpine Research*, 50(1), e1523638. Available from: <https://doi.org/10.1080/15230430.2018.1523638>
- Arrigo, K.R. (2017) Sea ice as a habitat for primary producers. In: Thomas, D.N. (Ed.) *Sea ice*, 3rd ed. Oxford, UK: Wiley-Blackwell, pp. 352–369.
- Barr, I., Dokukin, M., Koukoulos, I., Livingstone, S., Lovell, H., Małeck, J., et al. (2018) Using ArcticDEM to analyse the dimensions and dynamics of debris-covered glaciers in Kamchatka, Russia. *Geosciences*, 8(6), 216. Available from: <https://doi.org/10.3390/geosciences8060216>

- Baurley, N.R., Robson, B.A. & Hart, J.K. (2020) Long-term impact of the proglacial lake Jökulsárlón on the flow velocity and stability of Breiðamerkjökull glacier, Iceland. *Earth Surface Processes and Landforms*, 45(11), 2647–2663. Available from: <https://doi.org/10.1002/esp.4920>
- Belart, J.M.C., Magnússon, E., Berthier, E., Pálsson, F., Aðalgeirsdóttir, G. & Jóhannesson, T. (2019) The geodetic mass balance of Eyjafjallajökull ice cap for 1945–2014: processing guidelines and relation to climate. *Journal of Glaciology*, 65(251), 395–409. Available from: <https://doi.org/10.1017/jog.2019.16>
- Benn, D.I., Warren, C.R. & Mottram, R.H. (2007) Calving processes and the dynamics of calving glaciers. *Earth Science Reviews*, 82(3–4), 143–179. Available from: <https://doi.org/10.1016/j.earscirev.2007.02.002>
- Bennett, G.L., Evans, D.J.A., Carbonneau, P. & Twigg, D.R. (2010) Evolution of a debris-charged glacier landsystem, Kviárjökull, Iceland. *Journal of Maps*, 6(1), 40–67. Available from: <https://doi.org/10.4113/jom.2010.1114>
- Ben-Yehoshua, D., Sæmundsson, Þ., Helgason, J.K., Belart, J.M.C., Sigurðsson, J.V. & Erlingsson, S. (2020) Paraglacial exposure and collapse of glacial sediment: the 2013 landslide onto Svínafellsjökull, southeast Iceland. *Earth Surface Processes and Landforms*, 47(10), 2612–2627. Available from: <https://doi.org/10.1002/esp.5398>
- Bjork, A.B., Kjær, K.H., Korsgaard, N.J., Khan, S.A., Kjeldsen, K.K., Andresen, C.S., et al. (2012) An aerial view of 80 years of climate-related glacier fluctuations in southeast Greenland. *Nature Geoscience*, 5(6), 427–432. Available from: <https://doi.org/10.1038/ngeo1481>
- Björnsson, H., Pálsson, F., Gudmundsson, S., Magnússon, E., Adalgeirsdóttir, G., Jóhannesson, T., et al. (2013) Contribution of Icelandic ice caps to sea level rise: trends and variability since the little ice age. *Geophysical Research Letters*, 40(8), 1546–1550. Available from: <https://doi.org/10.1002/grl.50278>
- Boy, M., Thomson, E.S., Acosta Navarro, J.-C., Arnalds, O., Batchvarova, E., Bäck, J., et al. (2019) Interactions between the atmosphere, cryosphere, and ecosystems at northern high latitudes. *Atmospheric Chemistry and Physics*, 19(3), 2015–2061. Available from: <https://doi.org/10.5194/acp-19-2015-2019>
- Bradwell, T., Sigurðsson, O. & Everest, J. (2013) Recent, very rapid retreat of a temperate glacier in SE Iceland. *Boreas*, 42(4), 959–973. Available from: <https://doi.org/10.1111/bor.12014>
- Buri, P., Pellicciotti, F., Steiner, J.F., Miles, E.S. & Immerzeel, W.W. (2016) A grid-based model of backwasting of supraglacial ice cliffs on debris-covered glaciers. *Annals of Glaciology*, 57(71), 199–211. Available from: <https://doi.org/10.3189/2016AoG71A059>
- Carrivick, J.L., Sutherland, J.L., Huss, M., Purdie, H., Stringer, C.D., Grimes, M., et al. (2022) Coincident evolution of glaciers and ice-marginal proglacial lakes across the southern Alps, New Zealand: past, present and future. *Global and Planetary Change*, 211, 103792. Available from: <https://doi.org/10.1016/j.gloplacha.2022.103792>
- Carrivick, J.L. & Tweed, F.S. (2013) Proglacial lakes: character, behaviour and geological importance. *Quaternary Science Reviews*, 78, 34–52. Available from: <https://doi.org/10.1016/j.quascirev.2013.07.028>
- Carrivick, J.L. & Tweed, F.S. (2016) A global assessment of the societal impacts of glacier outburst floods. *Global and Planetary Change*, 144, 1–16. Available from: <https://doi.org/10.1016/j.gloplacha.2016.07.001>
- Carrivick, J.L., Tweed, F.S., Sutherland, J.L. & Mallalieu, J. (2020) Toward numerical modeling of interactions between ice-marginal proglacial lakes and glaciers. *Frontiers in Earth Science*, 8, 577068. Available from: <https://doi.org/10.3389/feart.2020.577068>
- Chandler, B.M.P., Chandler, S.J.P., Evans, D.J.A., Ewertowski, M.W., Lovell, H., Roberts, D.H., et al. (2020a) Sub-annual moraine formation at an active temperate Icelandic glacier. *Earth Surface Processes and Landforms*, 45(7), 1622–1643. Available from: <https://doi.org/10.1002/esp.4835>
- Chandler, B.M.P., Evans, D.J.A., Chandler, S.J.P., Ewertowski, M.W., Lovell, H., Roberts, D.H., et al. (2020b) The glacial landsystem of Fjallsjökull, Iceland: spatial and temporal evolution of process-form regimes at an active temperate glacier. *Geomorphology*, 361, 107192. Available from: <https://doi.org/10.1016/j.geomorph.2020.107192>
- Crochet, P., Jóhannesson, T., Jónsson, T., Sigurðsson, O., Björnsson, H., Pálsson, F., et al. (2007) Estimating the spatial distribution of precipitation in Iceland using a linear model of orographic precipitation. *Journal of Hydrometeorology*, 8(6), 1285–1306. Available from: <https://doi.org/10.1175/2007JHM795.1>
- Dell, R., Carr, R., Phillips, E. & Russell, A. (2019) Response of glacier flow and structure to proglacial lake development and climate at Fjallsjökull, south-east Iceland. *Journal of Glaciology*, 65(250), 321–336. Available from: <https://doi.org/10.1017/jog.2019.18>
- Dragosics, M., Meinander, O., Jónsdóttir, T., Dürig, T., De Leeuw, G., Pálsson, F., et al. (2016) Insulation effects of Icelandic dust and volcanic ash on snow and ice. *Arabian Journal of Geosciences*, 9(2), 126. Available from: <https://doi.org/10.1007/s12517-015-2224-6>
- Evans, D.J.A. & Orton, C. (2015) Heinabergsjökull and Skálafellsjökull, Iceland: active temperate piedmont lobe and outwash head glacial landsystem. *Journal of Maps*, 11(3), 415–431. Available from: <https://doi.org/10.1080/17445647.2014.919617>
- Ewertowski, M.W. & Tomczyk, A.M. (2015) Quantification of the ice-cored moraines' short-term dynamics in the high-Arctic glaciers Ebbabreen and Ragnarbreen, Petuniabukta, Svalbard. *Geomorphology*, 234, 211–227. Available from: <https://doi.org/10.1016/j.geomorph.2015.01.023>
- Eyles, N. (1979) Facies of supraglacial sedimentation on Icelandic and Alpine temperate glaciers. *Canadian Journal of Earth Sciences*, 16(7), 1341–1361. Available from: <https://doi.org/10.1139/e79-121>
- Fu, Y., Liu, Q., Liu, G., Zhang, B., Zhang, R., Cai, J., et al. (2022) Seasonal ice dynamics in the lower ablation zone of Dagongba glacier, southeastern Tibetan plateau, from multitemporal UAV images. *Journal of Glaciology*, 68(270), 636–650. Available from: <https://doi.org/10.1017/jog.2021.1231-15>
- Fugazza, D., Scaioni, M., Corti, M., D'Agata, C., Azzoni, R.S., Cernuschi, M., et al. (2018) Combination of UAV and terrestrial photogrammetry to assess rapid glacier evolution and map glacier hazards. *Natural Hazards and Earth System Sciences*, 18(4), 1055–1071. Available from: <https://doi.org/10.5194/nhess-18-1055-2018>
- García-Rodríguez, F., Piccini, C., Carrizo, D., Sánchez-García, L., Pérez, L., Crisci, C. et al. (2021) Centennial glacier retreat increases sedimentation and eutrophication in Subantarctic periglacial lakes: a study case of Lake Uruguay. *Science of The Total Environment*, 754, 142066. Available from: <https://doi.org/10.1016/j.scitotenv.2020.142066>
- Gindraux, S., Boesch, R. & Farinotti, D. (2017) Accuracy assessment of digital surface models from unmanned aerial vehicles' imagery on glaciers. *Remote Sensing*, 9(2), 186. Available from: <https://doi.org/10.3390/rs9020186>
- Girod, L., Nielsen, N.I., Couderette, F., Nuth, C. & Käb, A. (2018) Precise DEM extraction from Svalbard using 1936 high oblique imagery. *Geoscientific Instrumentation, Methods and Data Systems*, 7(4), 277–288. Available from: <https://doi.org/10.5194/gi-7-277-2018>
- Guðmundsson, S., Björnsson, H., Pálsson, F., Magnússon, E., Sæmundsson, Þ. & Jóhannesson, T. (2019) Terminus lakes on the south side of Vatnajökull ice cap, SE-Iceland. *Jökull*, 69(1), 1–34. Available from: <https://doi.org/10.33799/jokull2019.69.001>
- Gunnarsson, A., Gardarsson, S.M., Pálsson, F., Jóhannesson, T. & Sveinsson, Ó.G.B. (2020) Annual and interannual variability and trends of albedo for Icelandic glaciers. *The Cryosphere*, 15(2), 547–570. Available from: <https://doi.org/10.5194/tc-15-547-2021>
- Hannesdóttir, H., Björnsson, H., Pálsson, F., Aðalgeirsdóttir, G. & Guðmundsson, S. (2015a) Changes in the southeast Vatnajökull ice cap, Iceland, between ~1890 and 2010. *The Cryosphere*, 9(2), 565–585. Available from: <https://doi.org/10.5194/tc-9-565-2015>
- Hannesdóttir, H., Björnsson, H., Pálsson, F., Aðalgeirsdóttir, G. & Guðmundsson, S. (2015b) Variations of southeast Vatnajökull ice cap (Iceland) 1650–1900 and reconstruction of the glacier surface geometry at the little ice age maximum. *Geografiska Annaler: Series a, Physical Geography*, 97(2), 237–264. Available from: <https://doi.org/10.1111/geoa.12064>
- Hjaltason, S., Guðmundsdóttir, M., Haukdal, J.Á., & Guðmundsson, J.R. (2018) Energy statistics in Iceland 2017. *Energy Statistics in Iceland*, regimes at an active temperate glacier. *Geomorphology*, 361, 107192. Available from: <https://doi.org/10.1016/j.geomorph.2020.107192>

- Orkustofnun. Available at: <https://orkustofnun.is/gogn/Talnaefni/OS-2019-T009-01.pdf> (last access: 25 November 2022)
- Holland, M.M. & Bitz, C.M. (2003) Polar amplification of climate change in coupled models. *Climate Dynamics*, 21, 221–232. Available from: <https://doi.org/10.1007/s00382-003-0332-6>
- Holmlund, E.S. & Holmlund, P. (2019) Constraining 135 years of mass balance with historic structure-from-motion photogrammetry on Storglaciären, Sweden. *Geografiska Annaler: Series a, Physical Geography*, 101(3), 195–210. Available from: <https://doi.org/10.1080/04353676.2019.1588543>
- How, P., Schild, K.M., Benn, D.I., Noormets, R., Kirchner, N., Luckman, A., et al. (2019) Calving controlled by melt-under-cutting: detailed calving styles revealed through time-lapse observations. *Annals of Glaciology*, 60(78), 20–31. Available from: <https://doi.org/10.1017/aog.2018.28>
- Hugonnet, R., McNabb, R., Berthier, E., Menounos, B., Nuth, C., Girod, L., et al. (2021) Accelerated global glacier mass loss in the early twenty-first century. *Nature*, 592(7856), 726–731. Available from: <https://doi.org/10.1038/s41586-021-03436-z>
- Immerzeel, W.W., Kraaijenbrink, P.D.A., Shea, J.M., Shrestha, A.B., Pellicciotti, F., Bierkens, M.F.P., et al. (2014) High-resolution monitoring of Himalayan glacier dynamics using unmanned aerial vehicles. *Remote Sensing of Environment*, 150, 93–103. Available from: <https://doi.org/10.1016/j.rse.2014.04.025>
- IMO. (2022) The weather in Iceland in 2021. Report of the Icelandic Met Office (<https://en.vedur.is/about-imo/news/the-weather-in-iceland-in-2021>; last accessed on 12 December 2023)
- Ioli, F., Bianchi, A., Cina, A., De Michele, C., Maschio, P., Passoni, D., et al. (2022) Mid-term monitoring of glacier's variations with UAVs: the example of the belvedere glacier. *Remote Sensing*, 14(1), 28. Available from: <https://doi.org/10.3390/rs14010028>
- Jennings, S.J.A. & Hambrey, M.J. (2021) Structures and deformation in glaciers and ice sheets. *Reviews of Geophysics*, 59(3), e2021RG000743. Available from: <https://doi.org/10.1029/2021RG000743>
- Kavan, J. (2020) Early twentieth century evolution of Ferdinand glacier, Svalbard, based on historic photographs and structure-from-motion technique. *Geografiska Annaler. Series A, Physical Geography*, 102(3), 57–67. Available from: <https://doi.org/10.1080/04353676.2020.1715124>
- Kavan, J., Tallentire, G.D., Demidionov, M., Dudek, J. & Strzelecki, M.C. (2022) Fifty years of tidewater glacier surface elevation and retreat dynamics along the south-east Coast of Spitsbergen (Svalbard archipelago). *Remote Sensing*, 14(2), 354. Available from: <https://doi.org/10.3390/rs14020354>
- King, O., Dehecq, A., Quincey, D. & Carrivick, J. (2018) Contrasting geometric and dynamic evolution of lake and land-terminating glaciers in the central Himalaya. *Global and Planetary Change*, 167, 46–60. Available from: <https://doi.org/10.1016/j.gloplacha.2018.05.006>
- Kjær, K.H. & Krüger, J. (2001) The final phase of dead-ice moraine development: processes and sediment architecture, Kötlujökull, Iceland. *Sedimentology*, 48(5), 935–952. Available from: <https://doi.org/10.1046/j.1365-3091.2001.00402.x>
- Knudsen, Ó. (1995) Concertina eskers, Brúarjökull, Iceland: an indicator of surge-type glacier behaviour. *Quaternary Science Reviews*, 14(5), 487–493. Available from: [https://doi.org/10.1016/0277-3791\(95\)00018-K](https://doi.org/10.1016/0277-3791(95)00018-K)
- Magnússon, E., Pálsson, F., Björnsson, H. & Guðmundsson, S. (2012) Removing the ice cap of Öræfajökull central volcano, SE-Iceland: mapping and interpretation of bedrock topography, ice volumes, subglacial troughs and implications for hazards assessments. *Jökull*, 62(1), 131–150. Available from: <https://doi.org/10.33799/jokull2012.62.131>
- Małecki, J. (2021) Recent contrasting behaviour of mountain glaciers across the European high arctic revealed by ArcticDEM data. *The Cryosphere*, 16, 2067–2082. Available from: <https://doi.org/10.5194/tc-2021-165>
- Mallalieu, J., Carrivick, J.L., Quincey, D.J., Smith, M.W. & James, W.H.M. (2017) An integrated structure-from-motion and time-lapse technique for quantifying ice-margin dynamics. *Journal of Glaciology*, 63(242), 937–949. Available from: <https://doi.org/10.1017/jog.2017.48>
- Meinander, O., Dagsson-Waldhauserova, P., Amosov, P., Aseyeva, E., Atkins, C., Baklanov, A., et al. (2021) Newly identified climatically and environmentally significant high latitude dust sources. *Atmospheric Chemistry and Physics*, 22, 11889–11930. Available from: <https://doi.org/10.5194/acp-2021-963>
- Miles, E.S., Steiner, J., Willis, I., Buri, P., Immerzeel, W.W., Chesnokova, A., et al. (2017) Pond dynamics and supraglacial-englacial connectivity on debris-covered Lirung glacier, Nepal. *Frontiers in Earth Science*, 5, 69. Available from: <https://doi.org/10.3389/feart.2017.00069>
- Millan, R., Mouginot, J., Rabatel, A. & Morlighem, M. (2022) Ice velocity and thickness of the world's glaciers. *Nature Geoscience*, 15(2), 124–129. Available from: <https://doi.org/10.1038/s41561-021-00885-z>
- Möller, R., Dagsson-Waldhauserova, P., Möller, M., Kukla, P., Schneider, C. & Gudmundsson, M.T. (2019) Persistent albedo reduction on southern Icelandic glaciers due to ashfall from the 2010 Eyjafjallajökull eruption. *Remote Sensing of Environment*, 233, 111396. Available from: <https://doi.org/10.1016/j.rse.2019.111396>
- Motschmann, A., Huggel, C., Carey, M., Moulton, H., Walker-Crawford, N. & Muñoz, R. (2020) Losses and damages connected to glacier retreat in the Cordillera Blanca, Peru. *Climatic Change*, 162, 837–858. Available from: <https://doi.org/10.1007/s10584-020-02770-x>
- Nicholson, L. & Benn, D.I. (2013) Properties of natural supraglacial debris in relation to modelling sub-debris ice ablation. *Earth Surface Processes and Landforms*, 38(5), 490–501. Available from: <https://doi.org/10.1002/esp.3299>
- Noël, B., Aðalgeirsdóttir, G., Pálsson, F., Wouters, B., Lhermitte, S., Haacker, J.M., et al. (2022) North Atlantic cooling is slowing down mass loss of Icelandic glaciers. *Geophysical Research Letters*, 49(3), e2021GL095697. Available from: <https://doi.org/10.1029/2021GL095697>
- Özyeşil, O., Voroninski, V., Basri, R. & Singer, A. (2017) A survey of structure from motion. *Acta Numerica*, 26, 305–364. Available from: <https://doi.org/10.1017/S096249291700006X>
- Phillips, E., Everest, J., Evans, D.J.A., Finlayson, A., Ewertowski, M., Guild, A., et al. (2017) Concentrated, 'pulsed' axial glacier flow: structural glaciological evidence from Kviárjökull in SE Iceland. *Earth Surface Processes and Landforms*, 42(13), 1901–1922. Available from: <https://doi.org/10.1002/esp.4145>
- Porter, C., Morin, P., Howat, I., Noh, M.-J., Bates, B., Peterman, K., Keesey, S., Schlenk, M., Gardiner, J., Tomko, K., & Willis M. (2018). ArcticDEM. Harvard Dataverse, V1. Polar Geospatial Center, University of Minnesota. <https://doi.org/10.7910/DVN/OHHUKH>
- RGI Consortium. (2017) Randolph Glacier Inventory - A Dataset of Global Glacier Outlines, Version 6. Boulder, Colorado, USA: National Snow and Ice Data Center (NSIDC). Available from: <https://doi.org/10.7265/4m1f-gd79>
- Spedding, N. & Evans, D.J.A. (2002) Sediments and landforms at Kviárjökull, southeast Iceland: a reappraisal of the glaciated valley landsystem. *Sedimentary Geology*, 149(1–3), 21–42. Available from: [https://doi.org/10.1016/S0037-0738\(01\)00242-1](https://doi.org/10.1016/S0037-0738(01)00242-1)
- Statistics Iceland. (2021) Available at <https://www.statice.is/publications/news-archive/tourism/tourism-satellite-accounts-2018-2019/>. Accessed 25 November 2022.
- Sutherland, J.L., Carrivick, J.L., Gandy, N., Shulmeister, J., Quincey, D.J. & Cornford, S.L. (2020) Proglacial lakes control glacier geometry and behavior during recession. *Geophysical Research Letters*, 47(19), e2020GL088865. Available from: <https://doi.org/10.1029/2020GL088865>
- Swift, D.A. & Jones, A.H. (2018) Going against the flow: testing the hypothesis of pulsed axial glacier flow. *Earth Surface Processes and Landforms*, 43(13), 2754–2761. Available from: <https://doi.org/10.1002/esp.4430>
- Taylor, L.S., Quincey, D.J. & Smith, W.M. (2023) Evaluation of low-cost raspberry pi sensors for structure-from-motion reconstructions of glacier calving fronts. *Natural Hazards and Earth System Sciences*, 23(1), 329–341. Available from: <https://doi.org/10.5194/nhess-23-329-2023>

- Thórarinnsson, S. (1956) On the variations of Svinafellsjökull, Skaftafellsjökull and Kvíárjökull in Öræfi. *Jökull*, 6(1), 1–15. Available from: <https://doi.org/10.33799/jokull1956.06.001>
- Tsutaki, S., Fujita, K., Nuimura, T., Sakai, A., Sugiyama, S., Komori, J., et al. (2019) Contrasting thinning patterns between lake- and land-terminating glaciers in the Bhutanese Himalaya. *The Cryosphere*, 13(10), 2733–2750. Available from: <https://doi.org/10.5194/tc-13-2733-2019>
- Wang, P., Li, H., Li, Z., Liu, Y., Xu, C., Mu, J., et al. (2021) Seasonal surface change of Urumqi glacier no. 1, Eastern Tien Shan, China, revealed by repeated high-resolution UAV photogrammetry. *Remote Sensing*, 13, 3398. Available from: <https://doi.org/10.3390/rs13173398>
- Watson, C.S., Kargel, J.S., Shugar, D.H., Haritashya, U.K., Schiassi, E. & Furfaro, R. (2020) Mass loss from calving in Himalayan proglacial lakes. *Frontiers in Earth Science*, 7, 342. Available from: <https://doi.org/10.3389/feart.2019.00342>
- Welling, J. & Abegg, B. (2021) Following the ice: adaptation processes of glacier tour operators in Southeast Iceland. *International Journal of Biometeorology*, 65, 703–715. Available from: <https://doi.org/10.1007/s00484-019-01779-x>
- Wuite, J., Libert, L., Nagler, T. & Jóhannesson, T. (2022) Continuous monitoring of ice dynamics in Iceland with Sentinel-1 satellite radar images. *Jökull*, 72(1), 1–20. Available from: <https://doi.org/10.33799/jokull2021.72.001>
- Zhong, Y., Liu, Q., Westoby, M., Nie, Y., Pellicciotti, F., Zhang, B. et al. (2022) Intensified paraglacial slope failures due to accelerating down-wasting of a temperate glacier in Mt. Gongga, southeastern Tibetan plateau. *Earth Surface Dynamics*, 10(1), 23–42. Available from: <https://doi.org/10.5194/esurf-10-23-2022>

SUPPORTING INFORMATION

Additional supporting information can be found online in the Supporting Information section at the end of this article.

How to cite this article: Kavan, J., Stuchlík, R., Carrivick, J.L., Hanáček, M., Stringer, C.D., Roman, M. et al. (2024) Proglacial lake evolution coincident with glacier dynamics in the frontal zone of Kvíárjökull, South-East Iceland. *Earth Surface Processes and Landforms*, 49(5), 1487–1502. Available from: <https://doi.org/10.1002/esp.5781>